

# ON THE ABSENCE OF BROAD FORBIDDEN EMISSION LINES IN THE LOW LUMINOSITY SEYFERT 1 NUCLEUS OF NGC 3227

NICK DEVEREUX

Department of Physics, Embry-Riddle Aeronautical University, Prescott, AZ 86301

*Draft version March 12, 2022*

## ABSTRACT

The absence of broad [O III]  $\lambda\lambda 4959, 5007$  forbidden emission lines is one of the key arguments cited in the published literature for the gas density exceeding the critical density;  $7 \times 10^5 \text{ cm}^{-3}$ , in the broad line region (BLR) of active galactic nuclei. However, for NGC 3227, an equally valid alternative explanation is that  $\text{O}^{2+}$  is progressively ionized to  $\text{O}^{3+}$  as the central UV–X-ray source is approached. Observational evidence for such an ionization gradient is provided by spectra obtained with the *Space Telescope Imaging Spectrograph*. Modeling the rich UV–visible spectrum of NGC 3227 with the photoionization code Cloudy supports the interpretation that the absence of broad [O III] forbidden emission lines is due to ionization, rather than high gas density, and further suggests that what we perceive as the BLR in NGC 3227 is just the illuminated portion of a much larger inflow. The low metallicity deduced for the inflowing gas suggests an origin in the circumgalactic medium.

*Subject headings:* galaxies: Seyfert, galaxies: individual (NGC 3227), quasars: emission lines

## 1. PROLOGUE

This paper was rejected from two prestigious journals. Just as well as the Cloudy modeling results reported herein are highly uncertain because Cloudy has a bug in it. I had not discovered the bug until after I had written & submitted this manuscript. The bug is described in more detail in the forthcoming ApJ paper <http://adsabs.harvard.edu/abs/2015arXiv151204604D>. On a positive note, the observational results reported in this paper are correct, in particular the HST emission line fluxes. I think the reason that the manuscript was rejected is because of the idea expressed that photoionization, rather than gas density, is the reason for the absence of broad forbidden emission lines. Evidently, this possibility touched a raw nerve among the reviewers. However, that idea is expressed again in the aforementioned ApJ paper that will be published in 2016.

## 2. INTRODUCTION

A basic tenet with regard to the astrophysics of active galactic nuclei (AGN) is that the Hydrogen (H) gas number density in the broad line region (BLR) must exceed  $10^6 \text{ cm}^{-3}$  because of the absence of broad forbidden lines. The genesis of this widely held sentiment can be traced to Khachikyan & Weedman (1971), and Shields, Oke & Sargent (1972), who argued that ‘high density rather than high ionization is responsible for the absence of broad components to the forbidden lines’ in the Seyfert 3C 120. Specifically, the gas number density in the BLR must exceed the critical density of  $7 \times 10^5 \text{ cm}^{-3}$  for collisional de-excitation of the  $^1D_2$  level that would otherwise produce broad [O III]  $\lambda\lambda 4959, 5007$  forbidden emission lines<sup>1</sup>.

devereux@erau.edu

<sup>1</sup> Interestingly, the critical density is higher,  $2 \times 10^7 \text{ cm}^{-3}$ , for the  $^1S_0$  level responsible for the [O III]  $\lambda 4363$  forbidden emission line (Rubin 1989) but, unfortunately, this line is weak in NGC 3227 and the line profile shape is overwhelmed by emission from the red wing of the broad H $\gamma$  line (see Devereux 2013, for details).

However, in the case of NGC 3227, a contrary argument can be made that the  $\text{O}^{2+}$  ions required for the production of broad [O III] forbidden emission lines are absent because they have been ionized to  $\text{O}^{3+}$ . This reasoning follows from the observation that broad permitted C IV  $\lambda 1549$  line emission is ubiquitous in AGNs including NGC 3227 (Sulentic et al. 2007, and references therein). Permitted C IV  $\lambda 1549$  line emission results from collisionally excited  $\text{C}^{3+}$  ions which implies photons with energies exceeding the 48 eV required to ionize  $\text{C}^{2+}$ . With a similar ionizing potential of  $\sim 55$  eV,  $\text{O}^{2+}$  would also be ionized to  $\text{O}^{3+}$  yielding [O IV] line emission. Indeed, a bright [O IV] emission line is seen in NGC 3227 at  $25.9 \mu\text{m}$  as reported by Dasyra et al. (2011) although the limited angular resolution of the *Spitzer Space Telescope* prevents a definitive measurement of any BLR component. Nevertheless, it is conceivable that the coincidence of broad C IV emission and the absence of broad [O III] emission is due to high ionization rather than high density, contrary to widely held belief. To be fair, in defending collisional de-excitation as the explanation for the absence of broad [O III] emission lines in the Seyfert 3C 120, Shields, Oke & Sargent (1972) did acknowledge the caveat ‘unless X-ray ionization is important’. With hindsight we now know that broad line AGNs produce X-rays (Winter, Veilleux, McKernan & Kallman 2011, and references therein). Thus, photoionization of  $\text{O}^{2+}$  may well be the reason behind the absence of broad [O III] forbidden emission lines in NGC 3227, and, perhaps, other AGNs.

The purpose of this *Paper* is to report a new observational result, described in more detail in Section 2, which suggests that an ionization gradient exists in the central 1pc of NGC 3227. The new result is based on UV–visible spectroscopy obtained with the *Hubble Space Telescope* (*HST*). As discussed in Section 3, modeling the spectra using the photoionization code, Cloudy (Ferland et al. 2013), supports the interpretation that the absence of broad [O III] emission lines is due to ionization, not high

TABLE 1  
EMISSION LINE PARAMETERS FOR THE G140L AND G230L  
NUCLEAR SPECTRA OBTAINED 2–8–2000<sup>a</sup>

Line	Central Wavelength <sup>b</sup> Å	Flux <sup>c</sup> 10 <sup>-14</sup> erg cm <sup>-2</sup> s <sup>-1</sup>	FWHM kms <sup>-1</sup>
(1)	(2)	(3)	(4)
C IV <sup>d</sup>	1555 ± 1	≥ 7.4	4000
C III]	1913 ± 1	9.0 ± 0.3	4730 ± 207
Mg II <sup>d</sup>	2810 ± 3	≥ 11.5	2750
He II	1645 ± 1	1.4 ± 0.1	3070 ± 337

<sup>a</sup> Table entries that do not include uncertainties are fixed parameters.

<sup>b</sup> Observed wavelength

<sup>c</sup> Measured within a 0.2'' × 0.35'' aperture. Continuum subtracted but not corrected for dust extinction. Model dependent systematic uncertainties introduce an additional ~3% error not reported in the Table.

<sup>d</sup> The flux is a lower limit because emission line exhibits absorption features.

density, at least in NGC 3227. Conclusions are presented in Section 4.

### 3. RESULTS

The exquisite UV-visible spectra of the Seyfert 1.5 nucleus in NGC 3227 obtained with the Space Telescope Imaging Spectrograph (*STIS*) aboard *HST* have been presented most recently by Devereux (2013) and will not be discussed further here other than to say that Table 1 summarizes additional information for UV emission lines seen with the G140L and G230L gratings. Specifically, the vacuum wavelength Mg II  $\lambda$ 2798, C III]  $\lambda$ 1908, He II  $\lambda$ 1640 and C IV  $\lambda$ 1542 emission lines.

The evidence for an ionization gradient is presented in Figure 1 which illustrates a correlation between FWHM and ionization potential, separately for permitted, and forbidden lines in NGC 3227. The permitted lines show a similar range in ionization potential as the forbidden lines, although the ionization gradient for the forbidden lines is steeper. The significant velocity offset between the permitted and forbidden lines illustrates the conspicuous absence of broad forbidden lines in NGC 3227. In contrast to the correlation presented in Figure 1, there is no significant correlation between the FWHM and critical density for forbidden lines as illustrated in Figure 2.

### 4. DISCUSSION

An ionization gradient is expected in the nebula surrounding the central UV–X-ray source in NGC 3227 for the same reasons that one exists in the nebula surrounding H II regions and planetaries (Osterbrock & Ferland 2006). However, the exact nature of the ionization gradient depends on the ionizing spectrum of the central UV–X-ray source and the density of the surrounding gas all of which has been explored using version 13.02 of the photoionization modeling code, Cloudy (Ferland et al. 2013). Specific parameters employed to model the photoionization in NGC 3227 are listed in Table 2, and describe a spherically symmetric steady state inflow that is photoionized by the central UV–X-ray source. Following Vasudevan & Fabian (2009), the shape of the

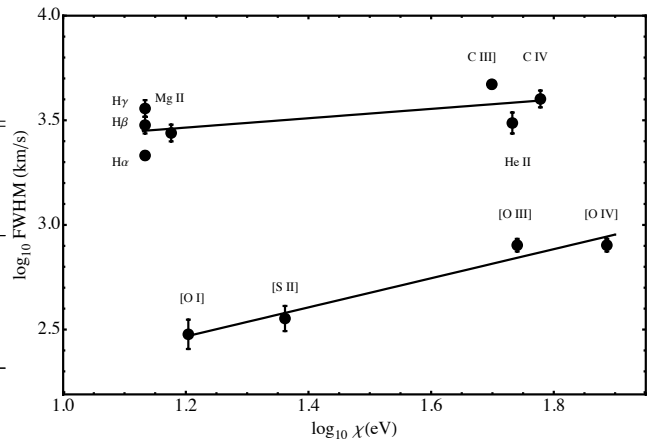


FIG. 1.— Correlation between FWHM and ionization potential for permitted, and forbidden emission lines in NGC 3227. Following Dasyra et al. (2011), the [O IV] data point has been included with a FWHM set equal to that of the [O III] line.

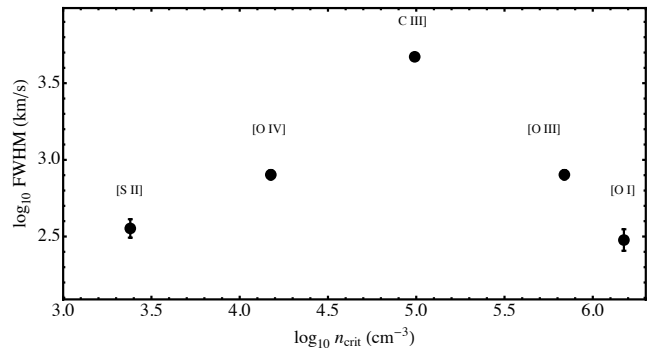


FIG. 2.— No correlation between FWHM and critical density for forbidden lines in NGC 3227. Following Dasyra et al. (2011), the [O IV] data point has been included with a FWHM set equal to that of the [O III] line.

ionizing spectrum is represented by the superposition of a 10<sup>5</sup> K blackbody, and a power law with spectral index  $\alpha_{\text{ox}} = -1.17$ . The number of ionizing photons,  $q(\text{h})$ , is constrained to be 52.8 dex (Devereux 2013). A spherical volume of neutral gas is described by an inner, and outer radius, and a radial density profile constrained by the requirement for a steady state inflow. The main attribute of the inflow model is that it can easily reproduce the shape of the single peak broad emission lines seen in NGC 3227 (Devereux 2013). Dust grain sublimation is also included. A full description of the parameters can be found in the Cloudy documentation.

#### 4.1. Ionization Structure of the Broad and Narrow Lines Regions.

Photoionization modeling of the inflow fueling the AGN in NGC 3227 yields the ionization structure illustrated in Figure 3 which was generated by Cloudy using the parameters listed in Table 2. The principal merits of this particular model are that the size of the H<sup>+</sup> region that is completely ionized coincides with the size of the BLR inferred from the shape of the broad H $\alpha$  emission line profile (see Devereux 2013), and identified in Figure 3 by the vertical dashed lines. Also, the ionization fraction progressively gives way to higher stages of ionization up to, and including O<sup>3+</sup>, as the central UV–X-ray source is approached suggesting an ionization gradient akin to the

TABLE 2  
INPUT PARAMETERS FOR THE CLOUDY PHOTOIONIZATION MODEL  
OF NGC 3227

Parameter
AGN T=1e5 K, $\alpha_{\text{ox}}=-1.17$
q(h)=52.8
radius 15.0 20.0
hden 8.95, power =-1.5
sphere
aperture slit
abundances ISM no grains
grains function sublimation
element scale factor carbon 0.1
element scale factor nitrogen 0.1
element scale factor oxygen 0.1
Stop temperature 2
iterations 2

one observed, and illustrated in Figure 1. Whilst only a proxy, the similar extent of the  $\text{O}^{2+}$  and  $\text{O}^{3+}$  regions may explain the similarity between the  $[\text{O III}]$  and  $[\text{O IV}]$  emission line profiles noted previously by Dasyra et al. (2011). However, since both lines are forbidden, they are susceptible to collisional de-excitation.

Cloudy predicts the electron density in the  $\text{O}^{\geq 2+}$  region to be  $10^4 \leq n_e (\text{cm}^{-3}) \leq 7 \times 10^5$ , which although is below the critical density for collisional de-excitation of the  $^1D_2$  level responsible for producing  $[\text{O III}]\lambda\lambda 4959, 5007$  forbidden emission lines, is significantly higher than the  $1.5 \times 10^4 \text{ cm}^{-3}$  critical density for the transition responsible for the  $25.9 \mu\text{m}$   $[\text{O IV}]$  emission line. Thus, Cloudy predicts the  $[\text{O IV}]$  emission line shape and intensity will be affected by gas density, but the same is not true for the  $[\text{O III}]\lambda\lambda 4959, 5007$  forbidden emission lines.

The ionization structure depends very sensitively on the density of the inflowing neutral H gas. Figure 3 illustrates the dependence in an animation consisting of a series of graphs for which the neutral H density at the reverberation radius;  $3.8 \text{ lt-days}$  or  $3.5 \times 10^{-3} \text{ pc}$  (Denney et al. 2010), is progressively increased from  $7.1 \leq \text{hden} \leq 8.3 \text{ dex}$ . Systematic trends are apparent, and are summarized as follows. First, as the neutral H density increases, the size of the  $\text{H}^+$  emitting region decreases as expected due to increased photoionization opacity. Indeed, when the neutral H gas density at the reverberation radius exceeds  $2 \times 10^8 \text{ cm}^{-3}$  the central UV–X-ray source is unable to photoionize an H nebula with any appreciable radial extent at all, and hence is unable to produce any broad H emission lines. Second, as the neutral H density increases, the  $\text{O}^{\geq 2+}$  and  $\text{C}^{\geq 2+}$  regions move progressively closer to the central UV–X-ray source, and diminish in size. Thirdly, as the neutral H density increases, the  $\text{O}^+$  and  $\text{O}^0$  regions move closer to the central UV–X-ray source which could result in broad vacuum wavelength  $[\text{O I}]\lambda\lambda 6302, 6365$  emission lines. The fact that broad  $[\text{O I}]$  emission lines are not observed (see Figure 1), even though the density in the  $\text{O}^0$  region is below the critical density,  $9 \times 10^5 \text{ cm}^{-3}$ , allows a firm constraint to be placed on the neutral H density for the inflowing gas;  $\text{hden} \leq 7.3 \text{ dex}$  at the reverberation radius. Since ionized H dominates the electron density,  $n_e \leq 7.3 \text{ dex}$  at the reverberation radius also. At larger radii,  $n_e$  asymptotes to  $\sim 3.65 \text{ dex}$ , close to the observed

value measured with the  $[\text{S II}]\lambda 6742/\lambda 6757$  ratio which corresponds to  $n_e \sim 10^3 \text{ cm}^{-3}$ , at a radial distance of  $\sim 0.5 \text{ pc}$ . Interestingly, the  $[\text{C III}]\lambda 1908$  line is a doublet, sensitive to gas density (Keenan, Feibelman, & Berrington 1992). In principle, the *Cosmic Origins Spectrograph* aboard *HST* could resolve the  $[\text{C III}]$  doublet in NGC 3227 providing an independent measure of the electron density inside the  $\text{O}^{\geq 2+}$  region because the  $\text{O}^{\geq 2+}$  and  $\text{C}^{\geq 2+}$  regions are predicted to be co-extensive (see Figure 3).

#### 4.2. Emission Line Ratios

What is visually striking about the spectra obtained with *STIS* of NGC 3227 is how weak the emission lines actually are compared to the H Balmer emission lines, especially the vacuum wavelength  $[\text{O II}]\lambda\lambda 3727, 3729$  lines which rendered NGC 3227 unclassifiable according to the diagnostic diagram of Kewley et al. (2006), as noted previously by Devereux (2013). Emission line ratios are a particularly sensitive diagnostic of the physical conditions in the ionized gas including the gas density, temperature and metallicity. Table 3 presents the observed emission line fluxes, normalized to  $\text{H}\beta$ , for multiple transitions of H, C, N, O, and S. When one compares the observed emission line ratios to the intrinsic values<sup>2</sup> predicted by the photoionization code Cloudy, the predicted emission line ratios for C, N, and O, are about one order of magnitude brighter than observed as shown in Table 3, and illustrated in Figure 4. The lines in question cover the gamut in wavelength, but the nature of the discrepancies are such that they can not be attributed solely to dust extinction. The differences are most apparent for the C, N and O lines, suggesting a metallicity dependence. Interestingly, as Figure 4 illustrates, the discrepancy between the observed and predicted values diminishes when the chemical abundance of C, N and O are decreased by a factor of ten compared to the ISM values quoted in the Cloudy documentation. Evidently, one explanation for the reason why the C, N and O emission lines are observed to be so faint in the AGN of NGC 3227 is because the gas there is metal poor, suggesting an origin in the circumgalactic medium. Perhaps the inflow, that we perceive as the BLR in NGC 3227, is just the terminus of a much larger inflow that originates from outside the galaxy. Such inflows of metal poor gas appear to be commonplace, observed in our own Galaxy (Bland-Hawthorn et al. 2007) and others (Lehner et al. 2013), but this is perhaps the first association between the BLR of an AGN and a low metallicity accretion flow from the circumgalactic medium. In the case of NGC 3227, the inflow may be facilitated by the interaction with NGC 3226 (Mundell et al. 1995, 1996).

#### 4.3. UV lines and Dust Extinction

The fact that the emission lines observed with *STIS* span such a large range in wavelength provides an opportunity to compare the dust extinction inferred from the emission lines with a prior study by Crenshaw et al. (2001) that employed the continuum. As Table 3 and Figure 4 illustrate, the good agreement between the

<sup>2</sup> employing the *aperture slit* option within Cloudy

TABLE 3  
COMPARING EMISSION LINE RATIOS

Line <sup>a</sup>	Observed Ratio <sup>b</sup>	Cloudy <sup>c</sup> C,N,O = 0.1 ISM	Cloudy <sup>c</sup> C,N,O = ISM
(1)	(2)	(3)	(4)
[S II] 6732	0.05	0.07	0.08
[S II] 6718	0.04	0.04	0.05
[N II] 6585	0.09	0.07	1.0
H $\alpha$ 6564	4.1	3.75	4.2
[N II] 6550	0.03	0.02	0.35
[O I] 6365	0.01	0.02	0.2
[O I] 6302	0.02	0.06	0.8
[O III] 5008	0.77	0.84	3.9
[O III] 4960	0.24	0.28	1.3
[O III] 4364	$\leq 0.02$	0.14	0.52
H $\beta$ 4862	1	1	1
H $\gamma$ 4341	0.3	0.46	0.47
[O II] 3727,3729	$\leq 0.01$	0.02	0.43
Mg II 2798	0.23	0.01	0.01
C III] 1908	0.18	3.4	15.3
He II 1640	0.03	5.23	4.46
C IV 1542	$\geq 0.15$	1.1	1.76

<sup>a</sup> Vacuum wavelength.

<sup>b</sup> Relative to H $\beta$ . Uncertainties in the observed ratio are  $\sim 10\%$ . Observed fluxes are measured within a  $0.2'' \times 0.35''$  aperture. They are continuum subtracted but not corrected for dust extinction. Model dependent systematic uncertainties introduce an additional  $\sim 3\%$  uncertainty not reported in the Table.

<sup>c</sup> Intrinsic values employing the aperture slit option within Cloudy.

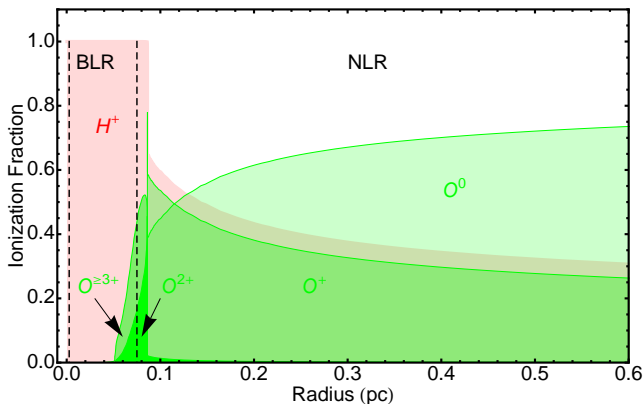


FIG. 3.— Photoionization model for NGC 3227. The radial dependence of the ionization fraction for H (pink shading), and various O ions (green shading) is shown in the top left panel. The radial dependence of the ionization fraction for H (pink shading), and various C ions (blue shading) is shown in the top right panel. The electron number density is shown in the lower left panel. The data point with the error bar represents the electron density measured using the [S II]  $\lambda 6742/\lambda 6757$  ratio which corresponds to  $n_e \sim 10^3 \text{ cm}^{-3}$ , at a radial distance of  $\sim 0.5 \text{ pc}$ . The neutral H number density,  $\propto r^{-3/2}$  is shown in the lower right panel. Vertical dashed lines identify the inner,  $r_i$ , and outer radii,  $r_o$ , of the BLR in units of pc (Devereux 2013). (An animation and a color version of this figure are available in the online journal.)

observed and predicted emission line ratios for the low metallicity gas suggests that the dust extinction to the visible lines is virtually negligible. The only exceptions are the vacuum wavelength C III]  $\lambda 1908$  and C IV  $\lambda 1542$  emission lines. Comparing the observed C IV/H $\beta$  emission line ratio with the intrinsic one predicted by Cloudy for the metal poor ISM leads to a differential extinction,  $A_{1542} - A_{H\beta} = 2.2 \text{ mag}$  which is lower than the  $3.8 \text{ mag}$

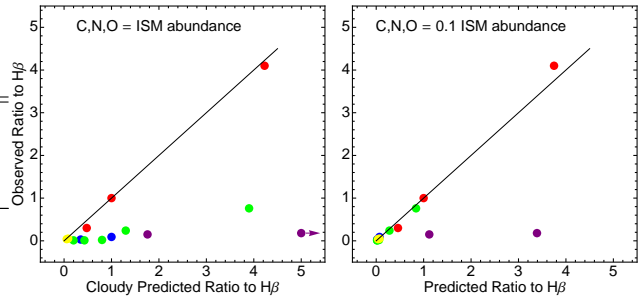


FIG. 4.— Comparing emission line ratios, normalized to H $\beta$ , for H (red), C (purple), N (blue), O (green) and S (Yellow) observed with *STIS* on the ordinate and those predicted by Cloudy on the abscissa (see Table 3). The left hand panel shows the correlation for emission line ratios predicted by Cloudy using ISM abundances. The right hand panel shows the correlation with emission line ratios predicted by Cloudy for gas that has been depleted in C, N, and O, by a factor of ten.

estimated using the extinction curve for NGC 3227 presented by Crenshaw et al. (2001). Indeed, the inferred dust extinction could be a further  $0.75 \text{ mag}$  smaller if one compensates for the fact that the C IV emission line suffers from intrinsic absorption (Crenshaw et al. 2001). On the other hand the differential extinction,  $A_{1908} - A_{H\beta}$ , estimated for the C III]/H $\beta$  emission line ratio is  $3.2 \text{ mag}$  which is higher than the  $2.5 \text{ mag}$  estimated using the extinction curve for NGC 3227 presented by Crenshaw et al. (2001). Taken together, the differences between the observed C III], and C IV line ratios, and those predicted by Cloudy, are inconsistent with a uniform screen of dust obscuration.

An additional puzzle involves the vacuum wavelength Mg II  $\lambda 2798$  emission line which is observed to be about a factor of 20 brighter than predicted by Cloudy, a situation that is only exacerbated by employing an extinction correction. However, the most remarkable discrepancy lies with the He II  $\lambda 1640$  line which is observed to be an order of magnitude fainter than predicted by Cloudy, even after correcting the observed line for a plausible  $3 \text{ mag}$  of extinction. The ions responsible for producing the Mg II  $\lambda 2798$  and He II  $\lambda 1640$  emission lines require photons with energies exceeding  $7 \text{ eV}$ , and  $54 \text{ eV}$  respectively. That these lines represent the extrema of ionization potentials sampled with the *STIS* spectra suggests that a remedy lies with the spectral shape adopted for the ionizing continuum. However, the discrepancy between the observed and predicted values for Mg II  $\lambda 2798$  and He II  $\lambda 1640$ , persists over a range in spectral index;  $-1.4 \leq \alpha_{\text{ox}} \leq -1.0$ , and blackbody temperatures;  $10^4 \leq T(\text{K}) \leq 3 \times 10^5$  selected for the Cloudy models.

The UV spectrum of NGC 3227 is also unusual when compared to other AGNs. For example, the C IV  $\lambda 1542$  emission line is much brighter than the adjacent C III]  $\lambda 1908$  emission line in the Sy 1 NGC 5548 (Korista & Goad 2000), and in nearby quasars (Negrete et al. 2013). Whereas in NGC 3227, the C IV  $\lambda 1542$  and C III]  $\lambda 1908$  emission lines are observed to be of comparable brightness.

In summary, the Cloudy photoionization model can successfully explain the relative intensities of the H, N, O and S emission lines seen in the visible, in terms of a low metallicity inflow photoionized by the central UV-X-ray source. However, the same model is unable to

simultaneously explain the UV emission lines, especially the bright Mg II  $\lambda 2798$  line, and the faint He II  $\lambda 1640$  line.

#### 4.4. Comparison with the Standard Broad Line Region Model

The main feature of the model presented here for NGC 3227 is photoionization of low density gas  $\leq 10^7 \text{ cm}^{-3}$  which leads to a spatially extended spherically symmetric nebula surrounding the central UV–X-ray source. In contrast, the so called ‘standard model’ for the BLR in Sy 1 nuclei and quasars refers to photoionization of high density gas;  $10^7 \text{ cm}^{-3} \leq n_e \leq 10^{14} \text{ cm}^{-3}$  (e.g., Kwan & Krolik 1981; Ferland et al. 1992; Korista & Goad 2000; Negrete et al. 2013). The main reason why the ‘standard model’ would fail to reproduce the UV–visible spectrum of NGC 3227 is because such high gas densities would quench the ionizing photons so completely that there would be no radial extent to the ionized nebula, and hence no broad emission lines, and no ionization gradient. As noted previously by Kwan (1984), a viable photoionization model must explain not only the emission line ratios but also the emission line shapes. As yet, there is no computer code that incorporates both photoionization and kinematics in such a way as to predict emission line shapes, but the development of such a capability is clearly the way forward to a complete understanding of the emission line spectra of AGNs, particularly given the wealth of information gathered with *STIS*.

In the case of NGC 3227, the broad emission lines allow the ionization structure of the photoionized nebula surrounding the AGN to be deciphered, empirically, by comparing the emission line profiles in velocity space as illustrated in Figure 5. The  $\text{H}\alpha$  profile defines the extent of the BLR in velocity space. The broad wings of the  $\text{H}\alpha$  line match those of the C IV profile. The two profiles depart at velocities with an absolute value less than 1000 km/s due to intrinsic absorption of the C IV line, attributed to foreground, low density, gas in the disk of this highly inclined galaxy (Crenshaw et al. 2001). However, the core of the C IV line is not important here, only the broad wings which the [O III] line does not have. By contrast with the C IV line, the [O III] line is narrow with no obvious broad component. Photoionization modeling with *Cloudy* suggests that the electron density in the  $\text{O}^{\geq 2+}$  region is below the critical density for collisional de-excitation of the  $^1D_2$  level responsible for producing [O III]  $\lambda 5007$  forbidden emission line (see section 3.1). Consequently, if one accepts that the C IV line provides a surrogate measure of the extent, in velocity space, of high ionization photons with energies  $\geq 48$  eV, then the reason why the broad wings of the C IV line

coincide with diminished [O III] line emission, is because  $\text{O}^{2+}$  is progressively ionized to  $\text{O}^{3+}$  as the central UV–X-ray source is approached. Such an ionization gradient is predicted by *Cloudy* (see Figure 3) and observed with *STIS* (see Figure 1).

## 5. CONCLUSION

This *Paper* presents evidence challenging the conventional wisdom that the absence of broad [O III] forbidden emission lines implies that the gas density is high enough,  $n_e \geq 7 \times 10^5 \text{ cm}^{-3}$ , to cause collisional de-excitation of the  $^1D_2$  level of  $\text{O}^{2+}$  in the BLR of AGNs. On the contrary, the absence of broad [O III] forbidden emission

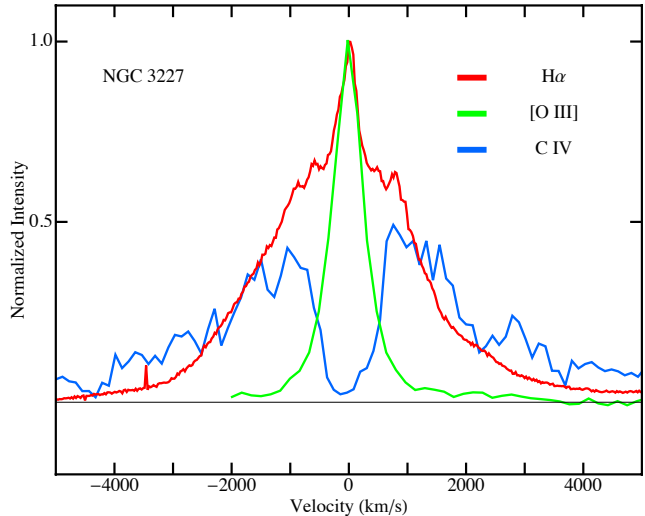


FIG. 5.— *HST* spectra showing a detailed comparison of the  $\text{H}\alpha$  (red), [O III] (green) and C IV (blue) emission line profile shapes with their respective wavelengths converted to velocity using the non-relativistic Doppler equation. The  $\text{H}\alpha$  and [O III] profiles are normalized to their respective peak intensity. The C IV profile is normalized, arbitrarily, to match the  $\text{H}\alpha$  profile at  $\pm 1300$  km/s.

lines is attributed to photoionization of  $\text{O}^{2+}$ , and not high density, at least in NGC 3227. The observational evidence includes an ionization gradient defined by a rich spectrum of UV–visible emission lines attributable to H, He, C, N, O, Mg, and S. Additionally, a comparison of emission line profile shapes reveals that high velocity permitted C IV  $\lambda 1549$  line emission coincides with diminished [O III]  $\lambda 5007$  forbidden line emission as would be expected if  $\text{O}^{2+}$  is progressively ionized to  $\text{O}^{3+}$ . These observational results constrain a model in which the central UV–X-ray source in NGC 3227 photoionizes a steady-state inflow of low metallicity gas.

## 6. ACKNOWLEDGMENTS

## REFERENCES

- Bland-Hawthorn, J., Sutherland, R., Agertz, O., & Moore, B., 2007, *apjl*, 670, 109
- Crenshaw D.M., Kraemer S.B., Bruhweiler F.C., Ruiz J.R., 2001, *ApJ* 555, 633
- Dasyra K. M., Ho L. C., Netzer H., Combes F., Trakhtenbrot B., Sturm, E., Armus L., Elbaz D., 2011, *ApJ* 740, 94
- Denney K.D., et al., 2010, *ApJ* 721, 715
- Devereux N., 2013, *ApJ* 764, 79
- Ferland G. J., Peterson B. M., Horne K., Welsh W. F. & Nahar S. N., 1992, *ApJ* 387, 95
- Ferland, G. J., Porter, R. L., van Hoof, P. A. M., Williams, R. J. R., Abel, N. P., Lykins, M. L., Shaw, G., Henney, W. J., and Stancil, P. C. The 2013 Release of *Cloudy*. *Revista Mexicana de Astronomia y Astrofisica*, 49, 137.
- Khachikyan E.Y., Weedman D. W., 1971, *Ap* 7, 231
- Kewley, L.J., Groves, B., Kauffmann, G., & Heckman, T., 2006, *MNRAS*, 372, 961
- Keenan, F. P., Feibelman, W. A., & Berrington, K. A., 1992, *ApJ*, 389, 443
- Korista K. T., Goad M. R., 2000, *ApJ* 536, 284
- Kwan J., 1984, *ApJ* 283, 70

- Kwan J., Krolik J. H., 1981, ApJ 250, 478
- Lehner, N., Howk, J. C., Tripp, T. M., Tumlinson, J., Prochaska, J. X., O'Meara, J. M., Thom, C., Werk, J. K., Fox, A. J., Ribaldo, J., ApJ, 770, 138
- Mundell, C. G., Pedlar, A., Axon, D. J., Meaburn, J., & Unger, S. W., 1995, MNRAS, 277, 641
- Mundell, C. G., Pedlar, A., Shone, D. L., Axon, D. J., Meaburn, J., & Unger, S. W., in Barred Galaxies, ASP Conference Series, Vol. 91, p.473
- Negrete C. A., Dultzin D., Marziani P., & Sulentic J. W., 2013, ApJ 771, 31
- Facilities:* HST (STIS)
- Osterbrock D., & Ferland G. J., 2006, Astrophysics of Gaseous Nebulae and Active Galactic Nuclei, 2nd ed. University Science Books, Sausalito, CA.
- Rubin R.H., 1989, ApJS 69, 897
- Shields G. A., Oke J. B., Sargent W. L. W., 1972, ApJ 176, 75
- Sulentic J. W., Bachev R., Marziani P., Negrete C. A., Dultzin D., 2007, ApJ 666, 757
- Vasudevan, R.V., & Fabian, A.C., 2009, MNRAS, 392, 1124
- Winter L.M., Veilleux S., McKernan B., Kallman, T.R., 2011, ApJ 745, 107